INVERSE MODELLING OF LAHENDONG GEOTHERMAL FIELD

Fajar Prasetyo[1], John O'Sullivan[1] and Michael O'Sullivan[1]

[1]Geothermal Institute and Department of Engineering Science, University of Auckland, New Zealand

m.osullivan@auckland.ac.nz

Keywords: *Lahendong geothermal field, inverse modelling, natural state modelling.*

1. ABSTRACT

Manual calibration to adjust parameters to produce a model that best represents the actual behaviour of a geothermal system is a tedious and frustrating process. This paper discusses automatic calibration of a geothermal reservoir model employing inverse modelling techniques. Inverse modelling simulators, namely PEST and iTOUGH2, are utilized to identify the values of parameters that achieve the best fit between the model results and the measured data for the natural state of Lahendong geothermal field.

There were two aims for the project: first, to develop an improved model of Lahendong, and second to establish good, general protocols for inverse modelling of geothermal reservoirs.

1. INTRODUCTION

Lahendong geothermal field is located in the northern arm of the K-shaped island of Sulawesi, Indonesia, approximately 30 km south of Manado, the capital city of North Sulawesi Province, at an elevation of 750 m above sea level (Fig. 1). Regionally, this field is located in the west margin of the Tondano Depression which extends about 20 km in the north-south direction and opens to the west. Within this depression is the Pangolombian rim, circular in shape, which is an important structure in Lahendong geothermal system (Koestono *et al*., 2010).

Lahendong is a liquid-dominated reservoir and is divided into two different zones based on reservoir temperatures: the southern zone with very high temperatures (350°C) and the northern zone with more modest temperatures (250°C) (Yani, 2006). This geothermal field was discovered in 1982 and geoscience investigations have been conducted ever since. Three shallow wells were drilled around Lake Linau in 1982 and seven exploration wells were drilled between 1982 and 1987. Wells LHD-1 and LHD-5 are in the northern zone, LHD-4 is in the southern zone and LHD-3, LHD-6 and LHD-7 are in the boundary margins of the prospect area (Koestono *et al*., 2010, after Robert, 1987). Development wells LHD-8 to LHD-16 were drilled between 1991 and 1998.

Lahendong geothermal field is producing 80 MW of electricity from 4 units. Unit-1 (1 x 20 MWe) was commissioned in 2001, followed by Unit-2, Unit-3 and Unit-4, each with 20 MWe capacity, commissioned in 2007, 2009 and 2012, respectively. The production rate for this field is around 1100 t/h, with 600 t/h of steam and 500 t/h of brine from 10 production wells. A cold reinjection system is employed in which brine and condensate are mixed in one reinjection line before being reinjected at one cluster, consisting of 3 injection wells (Prabowo *et al*., 2015). Unit-5 and Unit-6, each with 20 MWe capacity, are currently in the EPCC stage and are scheduled to be commissioned at the end of 2016. This field is likely to be further developed, with several make-up wells scheduled to be drilled, and hence it is important to understand the reservoir behavior.
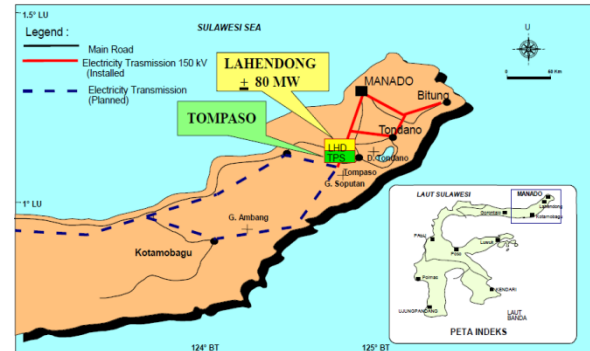
Figure 1: Location map for Lahendong geothermal field

Several reservoir modelling studies of Lahendong have been conducted, comparing the temperature distribution and flow of heat and fluid in the model with measured field data and then manually adjusting the permeability structure of the model to achieve a satisfactory match (Yani, 2006; Sumantoro *et al*., 2015; Brehme *et al*., 2016a,b).

The aim of the present study was to use inverse modelling to improve two models of Lahendong. The first (Model I) is essentially the same as that developed by Sumantoro *et al*. (2015). Inverse modelling was able to improve Model I but only up a point where some of the matches to downhole temperature profiles were still not very good. At this stage the conceptual model was reviewed using information from recent reports (e.g.: Widagda & Jagranatha, 2005; Siahaan *et al*., 2005; Utami *et al*., 2007; Koestono *et al*., 2010; Brehme *et al*., 2014, 2016ab) and a revised model, Model II, was set up. Then some manual calibration, followed by inverse modelling was used to improve Model II.

The overall goodness of fit of the model is measured by an objective function (OF), which is the sum of squares of the difference between modelled and measured downhole temperatures in all the wells for which data are available. Table 1 shows a summary of the improvement in the objective function achieved during the study. The fit to the data with final version of Model II achieved an OF two-thirds that for the best version of Model I.

Table 1: Improvement in the objective function

Model	Stage	Obj. Function
I	After manual calibration	0.2655E6
I	After inverse modelling	0.1578E6
II	After manual calibration	0.2571E6
II	After inverse modelling	0.1030E6

During the process of inverse modeling on Model I and Model II protocols were developed (discussed below) which may be applicable to inverse modelling of other geothermal systems.

2.   MODEL I

Lahendong geothermal field has been investigated by PT. PGE, the owner of the field for many years, and the subject of several internal reports. The first open-source report on modelling was by Yani (2006), who discusses a numerical model of Lahendong reservoir based on geological, geochemical, geophysical and well measurement data. Sumantoro *et al*. (2015) based their study on Yani's work but refined the model in several respects:

a) By extending the area of the model to 12 km x 12 km, and refining the grid to include 33 rows (NE-SW, "x" direction) and 33 columns (NW-SE, "y" direction), with a finer grid in the production and reinjection areas (see Fig. 2). The layer structure was refined to include 26 layers, the thinnest layer being 50 m and the thickest 300 m, giving a total of 20740 blocks (see Fig. 3)

b) By rotating the grid to the west by 28.9 degrees from north, in order to align the grid to the major fault in the area (NE-SW), thus giving a NE-SW orientation of the grid. The aligning of the grid with the fault helps in assigning the model parameters, such as setting one horizontal permeability to be higher than the other

c) By using real topographic data for the top layers at around 700-900 masl. The top layers are thinner than the deeper layers in order to more accurately represent the water table and the shallow unsaturated zone.
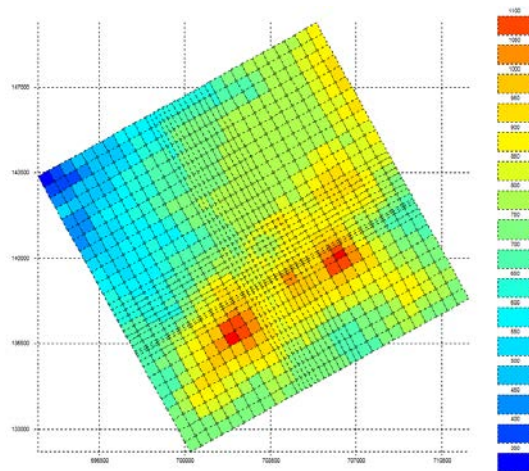

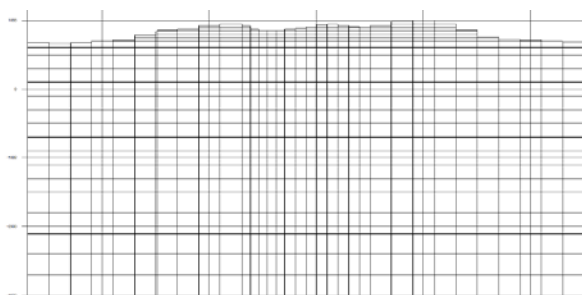**Figure 2: Plan view of Model I (Sumantoro *et al*., 2015)**

Figure 3: Layers in Model I (Sumatoro *et al.*, 2015)

All rocks and fault material in Sumantoro's model (called Model I here) were assumed to have rock density of 2500 kg/m^3, thermal conductivity of 2.5 W/m.K, specific heat of 1000 J/kg.K and a porosity of 10%. The permeability of each rock-type was assigned with initial value in the range 0.1-50 mD and was then determined by calibration (O'Sullivan *et al*., 2001).

The model boundary conditions used were:

▪ Atmospheric condition: The top layers are connected to atmosphere block, the "ATM 0", which remains at a stable temperature of 25°C and a pressure of 1 bar.
▪ An annual rainfall of 3.187 mm/year, based on actual rainfall data in Lahendong area, with an infiltration rate of 10%. Rainfall is represented in the model by an inflow of cold water into the top layer with an enthalpy of 104.8 kJ/kg.
▪ No-flow boundary conditions are assumed at all side boundaries, meaning no heat or mass coming into, or out of the system.
▪ A conductive heat flux of 80 mW/m^2 is applied across the whole system.
▪ Inflow of hot water into the bottom layer of 90 kg/s is distributed at several points around the potential production area. As suggested by the conceptual model, initially mass inflows were located mainly beneath LHD-1 and LHD-4. It was part of the model calibration process to determine the best locations for the hot inflow.
▪ The enthalpy of the deep mass flow varies from 1500-1800 kJ/kg.
▪ Maximum base temperature is 320°C.
▪ Several hot springs with a total mass flow of around 100 kg/s are also represented in the model.

The air-water, EOS3 equation of state module of TOUGH2 is used in both Model I and Model II so that the shallow unsaturated zone could be included in the model.

3.   INVERSE MODELLING

Parameter estimation, history matching, model calibration and inverse modelling are terms describing the same technique with slightly different objectives in mind. The ultimate goal of inverse modelling is to determine the best model and its parameters for predicting the behavior of a system. In geothermal modelling, assigning parameters is likely to be challenging because of the relatively large number of parameters that need to be specified, and the difficulties of measuring their values in the field (Finsterle, 2000).

The goodness of fit between the model results and observed data is quantified by an objective function. As mentioned above the OF used here is the sum of squares of the difference between modelled and measured downhole temperatures in all the wells for which data are available.

The optimization process is then performed, involving a number of iterations, to obtain the set of parameters that produces the lowest value of the objective function. In the present study the reservoir parameters used are the permeabilities and deep inflows of hot water at the base of the model. The measured field data used as observations are temperature profiles in the wells. In inverse modelling, results calculated by the model are matched to the set of field data by adjusting model parameters.

There are three key elements of an inverse modelling study:

2

1) A numerical simulator capable of solving the forward model.
2) An objective function measuring the overall difference between observed data and the corresponding simulation results.
3) A minimization algorithm for reducing the objective function, by systematically updating parameter values.

TOUGH2 (Pruess *et al.*, 1999) or AUTOUGH2, the University of Auckland's version of TOUGH2 (Yeh *et al.*, 2012), is the forward simulator used in this project, while two inverse modelling simulators are used to perform model calibration, namely: iTOUGH2 and PEST.

3.1 iTOUGH2

iTOUGH2 (inverse TOUGH2 – Finsterle, 2000) is a computer program that provides inverse modelling capabilities for the TOUGH2 codes. iTOUGH2 is capable of supporting three investigation modes: parameter estimation, sensitivity analysis and uncertainty propagation analysis.

iTOUGH2 estimates the parameters by automatically adjusting them to achieve the best fit between the calculated output and the observed data. A number of different objective function options and minimization algorithms are available for the user to specify. iTOUGH2 allows automated parameter estimation to replace the otherwise tedious work of trial-and-error model calibration. The sensitivity analysis has a practical significance as it identifies the parameters that most significantly affect the model output. The uncertainty propagation analysis provides insight into the uncertainty of the estimated parameters and reveals parameter correlations.

Two input files are needed to run iTOUGH2:

(i) A TOUGH2 input file based on the conceptual model, which for Model I is the input file developed by Sumantoro *et al.* (2015).

(ii) An iTOUGH2 input file, in which the modeler specifies the parameters to be estimated and the data used for calibration.

A standard TOUGH2 forward run should be performed in order to check the appropriateness of the simulation prior to starting more time-consuming inversion. Plotting the model output with the initial parameter set against the data is strongly recommended so that errors such as wrong conversion factors, opposite signs of measured and calculated flow rate, data shifts etc. can be detected. It also provides a first assessment of the model and allows the modeler to estimate the time required to solve the inverse problem (Finsterle, 2000). Graphical interface software can be used to visualize the output from TOUGH2 or AUTOUGH2. MULgraph and TIM are the most common tools used at the University of Auckland (Yeh *et al.*, 2013).

3.2 PEST

PEST, an acronym for Parameter ESTimation, is a set of programs for parameter estimation, sensitivity analysis and uncertainty propagation analysis (Doherty, 2005). PEST uses a computer model to predict the real system behavior and adjusts model parameters until an optimum fit between the model output and field observation data is reached.

The universal applicability of PEST lies in its model independence, i.e., its ability to automatically adjust the model parameters to fit the model output with the field observation data for any model. PEST requires that the forward model can read input data from one or a number of ASCII input files and writes the outcomes of its calculations to one or more ASCII output files. Thus a model does not have to be rewritten as a subroutine and recompiled before it can be used within a parameter estimation process. Just as Doherty (2005) states: PEST adapts the model, the model does not need to adapt to PEST.

PEST offers several advantages over the other inverse modelling simulators: PEST is free, well documented, fully supported and the source code is publicly available. PEST, especially the parallel version, is multi-platform, and hence works equally well on both Windows and Linux operating systems. Any computer connected through a local area network or wireless network can be used to construct a parallel environment, without the necessity of having a specialized cluster of parallel computers. Groups of multiple computers, possibly running multiple cores, can participate in the parallel PEST mode without any need for special configuration. Finally, PEST runs in a script-like manner, being model-independent, which enables a modeler to use it without modification of an existing forward model simulation code. It only works on the input and output files and the sole role of the forward simulator is to accept the input file, carry out a model calculation and produce the output file.

PEST uses an algorithm called Gauss-Marquardt-Levenberg (also available in iTOUGH2). The strength of this method lies in the fact that it can generally estimate parameter using fewer model runs than any other estimation method, a definite bonus for large models whose run-times may be very large (Doherty, 2005).

PEST requires the use of three primary input files, namely a template file, an instruction file and a control file (Doherty, 2005). The use of these three files enables PEST to access model input and output files without having to know how the modelling simulator works (see Fig. 4). It simply attaches itself to the input file creation and output file extraction process normally carried out by the user.
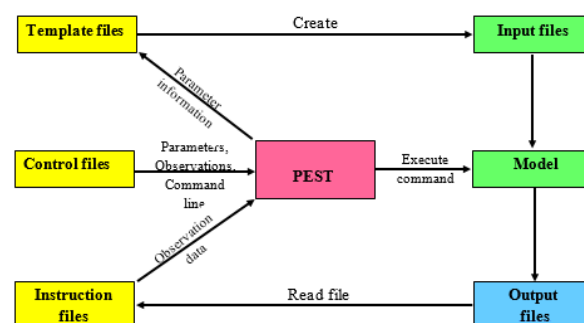
**Figure 4: Simplified diagram of the PEST optimization process**

4. RESULTS FOR MODEL I

4.1 Manual calibration

Manual calibration of Model I was performed by Sumantoro *et al.* (2015) in order to improve the match of model results to the field temperature profiles, by manually adjusting the magnitude and enthalpy of the deep mass inflows, adjusting the permeability of the rock-types, adding new rock-types and introducing new faults. Fig. 5 shows some of the final

3

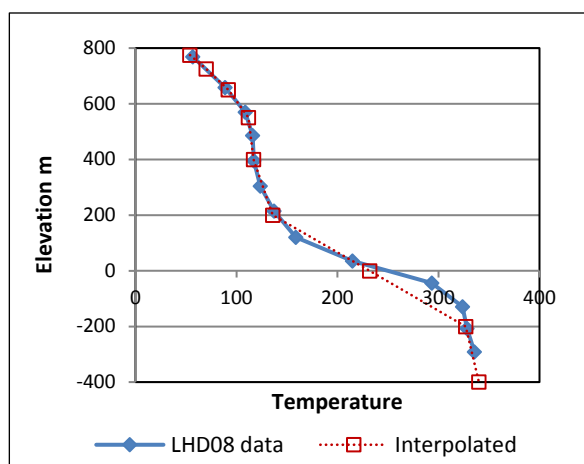temperature profiles for Model I obtained after manual calibration.
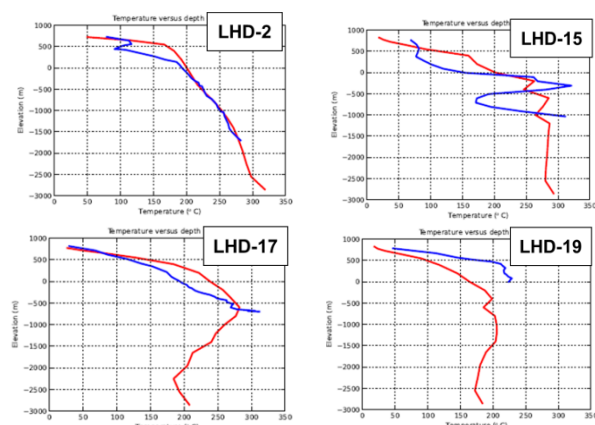
Figure 5: Temperature profiles for Model I after manual calibration. Wells LHD-2, LHD-15, LHD-17 and LHD-19

As shown in Fig. 5 above, a good match between the model output and the field data was obtained, although there is still room for further improvements. In the next stage of the project the model was improved by utilizing inverse modelling techniques.

4.2   Inverse modelling

In the first part of the study, parameter estimation was performed for two sets of parameters: x,y,z permabilities for 30 rock-types (90 parameters) and mass flow rates at 25 deep inflows., giving a total of 115 parameters.

The observations used in this project were temperature profiles from 16 exploration and exploitation wells in Lahendong. To use the data, first the corresponding blocks in the model through which the wells pass were located, and then the field data were interpolated on to the block centres (see Fig. 6). The block names and the corresponding observed (interpolated) temperatures were used as observations in iTOUGH2 and PEST.

Figure 6: Field data and temperatures interpolated to block centres for well LHD-8.

Many inverse modelling runs were performed with both iTOUGH2 and PEST. The results obtained with iTOUGH2 and PEST were very similar and only the iTOUGH2 results are presented here. As shown in Table 1 inverse modelling improved Model I, with the objective function dropping

from 0.2655E6 after manual calibration to 0.1578E6 after inverse modelling. Some of the results obtained after inverse modelling are shown in Fig. 7. As expected a comparison with Fig. 5 shows that they have improved.
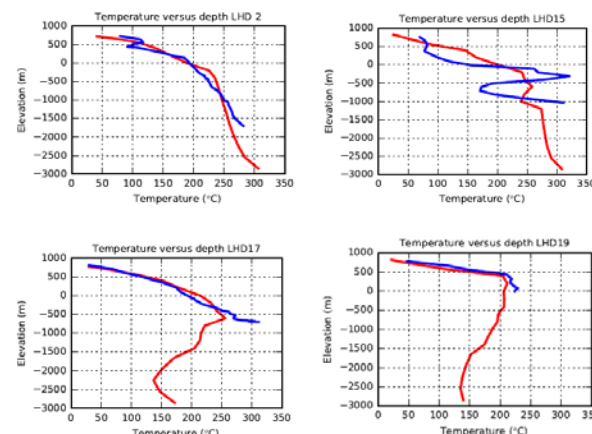
Figure 7: Temperature profiles for Model I after calibration with iTOUGH2

As well as obtaining an improved version of Model I our inverse modelling experiments helped to establish some protocols that we adopted with inverse modelling of Model II (discussed below) and which may have general application to inverse modelling of any geothermal system. We discuss these finding under several headings below.

Convergence of the natural state. We found it to be very important that each forward simulation reached a stable natural state with a large simulation time (1.0E15 s). To ensure that this happens it is necessary to make sure that at least one Newton-Raphson update is made at each time-step of the forward TOUGH2 simulation. This was achieved by setting MOP2(1)=2 in the TOUGH2 data file.

If this option was not used many of the forward, TOUGH2, simulations finished before the target simulation time and then the parameter update after an outer iteration of iTOUGH2 was not satisfactory and the forward simulations during the second outer iteration of iTOUGH2 performed very badly. Note that an outer iteration of iTOUGH2, used for parameter updating, requires NP+1 simulations, i.e., forward runs, with TOUGH2, where NP is the number of model parameters to be estimated.

Parameter bounds. With iTOUGH2 or PEST the user sets bounds within which the parameter value is required to stay. As inverse modelling proceeds the sensitivity of parameters is calculated. It is a measure of how much the particular parameter affects the objective function, i.e., the fit of the model results to the data. Parameters with a very low sensitivity tend to move to their upper or lower bounds. If bounds are set too high or too low this phenomenon tends to create models with large permeability contrasts that converge slowly (or not at all) to the steady, natural state.

In our early experiments with inverse modelling of Lahendong we used bounds of 1.0E-17 m^2 and 1.0E-11 m^2 for permeability but then some forward model runs converged very slowly. However, with bounds on permeability of 1.0E-16 m^2 and 2.0E-12 m^2 convergence was satisfactory.

4

Manual intervention. Typically, in an iTOUGH2 simulation the first outer iteration reduces the objective function by 10-20% but subsequent outer iteration reduce the OF by much less. We found it to be effective to stop iTOUGH2 after the first outer iteration and remove all parameters with a low sensitivity (say less than 0.1 - important parameters have sensitivities in the range 10-100) and those that had reached a lower or upper bound (often these had a low sensitivity). Then iTOUGH2 was restarted using updated parameter values except for the non-influential parameters whose values were left at the bound or re-set to a reasonable value based on expert knowledge.

Two or three iterations of this process, eliminating parameters at each stage, required less time than just letting the original iTOUGH2 simulation run for several outer iterations.

Staged inversion. As pointed out above if there are NP model parameters each outer iteration of iTOUGH2 requires NP+1 forward simulations with TOUGH2, and a general aim with inverse modelling is to reduce the number of model parameters. We therefore experimented with a two stage process where we included only permeabilities in the first stage and followed the processes discussed above to eliminate all permeabilities with a low sensitivity. We then added in the mass flows as parameters for the second stage but now using many fewer permeabilities as parameters.

A similar idea was used with inverse modelling of Model II (discussed below) which has many more rock-types than Model I (86 versus 30). In this case the two horizontal permeabilities (k_x and k_y) were assumed to be equal, thus reducing the number of permeability parameters from 258 down to 172. Then, following our manual intervention strategy, after the first outer iteration of iTOUGH2 a k_x/k_y parameter with a low sensitivity was removed and that with a high sensivity was split into separate k_x and k_y parameters.

5. IMPROVED MODEL OF LAHENDONG GEOTHERMAL FIELD – MODEL II

5.1 Rationale

The results discussed in the previous section showed that inverse modelling was effective in improving Model I but the optimized version of the model are still not as good as we wished to achieve, and which we expected a long period of manual calibration could achieve. The problem is that inverse modelling can only produce the best version of the model given the assumed rock-type distribution and distribution of the deep inflows. Thus to improve the model of Lahendong further required a revision of its structure.

Hence, it was thought to be worthwhile to revisit the conceptual model of Lahendong geothermal field and build a better and more physically correct model. Two aspects of the model that were investigated particularly were the faults and the location of the clay cap.

5.2 Conceptual Model

Lahendong is located in Tomohon City about 30 km to the south of Manado City, the capital of North Sulawesi Province, on the northern arm of Sulawesi. The topography of the area is characterized by volcanoes and lakes. Mount Tampusu, Mount Lengkoan, Mount Lokon and Mount Soputan rise as high as 1150 masl and form the volcanic inner-arc of Minahasa. Lake Linau, an acid lake of pH 2.7, is

located at 780 masl. (Siahaan *et al*., 2005; Brehme *et al*., 2014).
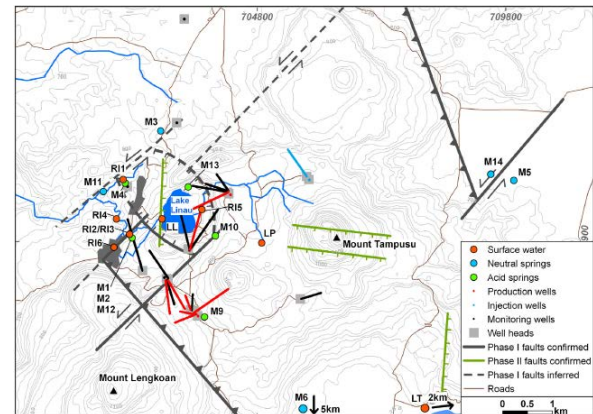

Figure 8: Lahendong geothermal field showing wells and their location relative to faults (from Brehme *et al*., 2014)

The regional geology of the Northern arm of Sulawesi is divided into 3 compartments which are the central E-W trending segment (Gorontalo compartment), the N-S trending compartment and the NE-SW trending compartment (Minahasa compartment). This structure is influenced by the double seduction of the Molucca plate beneath Sangihe ridge (Siahaan *et al*., 2005).

The main geologic structures are: Pangolombian caldera, Linau crater, NE-SW trending faults, NW-SE trending faults, E-W trending faults and N-S trending faults (Utami *et al*., 2004; Koestono *et al*., 2010). These faults play a major role in controlling the fluid flow of the field (Yani, 2006).

The geothermal clay cap of the field is characterized by low resistivity. A detailed MT survey followed by a 3D MT inversion confirmed the existence of an updome resistivity structure, with an upwelling region situated under Lake Linau (Raharjo *et al*., 2010). Three slices at different depth, shown in Figure 9, help to visualize the dome. At shallow depth, the conductor layer is concentrated in the vicinity of Lake Linau (Figure 9 (a)), located between elevations of 475 to 600 masl, with an approximate area of 5x5 km^2.
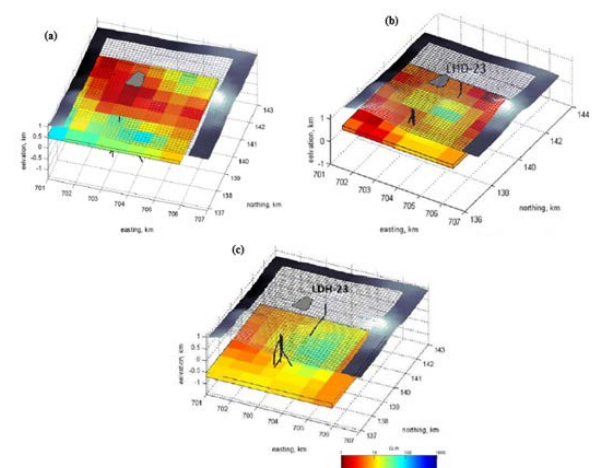
Figure 9: 3D view of the resistivity structure of Lahendong at elevations of: (a) 475-600 masl; (b) 40-200 masl; (c) -700 to -500 masl (taken from Rahardjo *et al*., 2010)

5

At a slightly greater depth (elevation 40 to 200 masl), the conductor layer extends wider, with an elongated shape trending ENE-WSW and curling to the south at the southern end. While at a greater depth of around 1.4 km the size of the dome is about 3 x 4 km^2. It is more or less circular under the lake and extends to the south. These three slices shows the dome-like structure of the resistivity anomaly with a steeper side in the north and a gentler side in the south.

5.3   Design of Model II

The new model, Model II, covers a slightly larger area than Model I (13 km x 13m rather than 12km x12km). A fine grid is used at the center of the model where most of the wells are located while coarser blocks are used in the surrounding area to reduce the total number of blocks in the model (see Fig. 10). The area covered by small blocks is larger for Model II than for Model I but the largest blocks at the outer parts of Model II are larger (1000 m x 1000m vs 500 m x 500 m). Model II has 979 blocks per layer and a total of 14458 blocks whereas Model I has 1089 blocks per layer and a total of 20740 blocks. Both models have 26 layers (see Fig. 11).

Topographical data is used to set the elevation of the top of each column while the base of the model is set at an elevation of 3000 mbsl, more than 1300 m deeper than the maximum depth penetrated by the deepest well used in this project, LHD02, whose bottom-hole is located at -1700 mbsl.
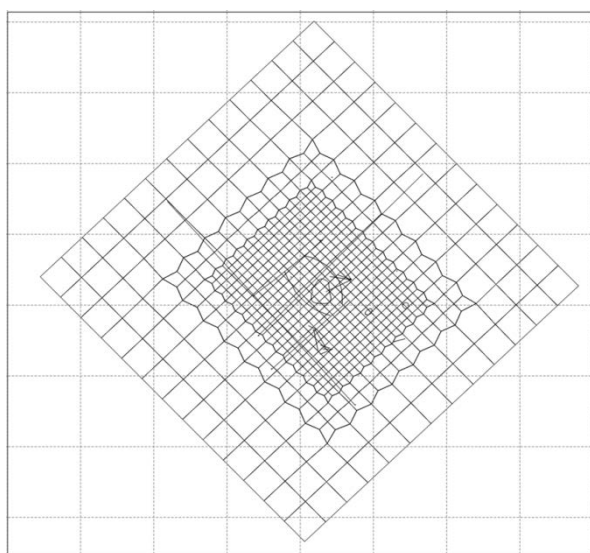
**Figure 20: Plan view of Model II**
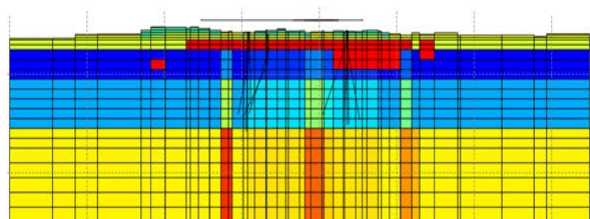
Figure 31: Vertical layers in Model II

The main geological structure in the field, i.e. faults, a crater and a caldera, are incorporated into the numerical model and are given their own rock-types. As for Model I, all rock-types were assigned a rock density of 2500 kg/m^3, a thermal

conductivity of 2.5 W/m.K, a specific heat of 1000 J/kg.K and a porosity of 10%.

Most of boundary conditions used in Model II are the same as for Model I but the deep hot inflow is distributed more widely. For the starting point of model calibration, 81 blocks along the faults were assigned mass upflows in the range of 0.25 – 1 kg/s. The distribution of mass input used for the model is shown in Fig. 12.
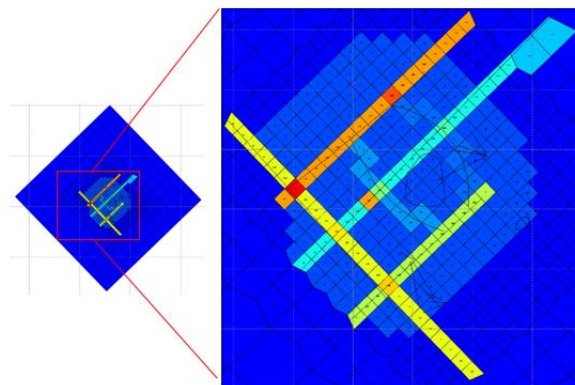

Figure 42: Initial mass inflows at the base of Model II

The basic rock-type structure from Model I was carried over to Model II and then the faults, crater, caldera and clay cap were assigned. A total of 86 rock-types were used in the model.

One of the important improvements in Model II was the inclusion of a cap rock in the model based on the resistivity structure shown in Fig. 9. However some extrapolation and smoothing was applied to establish a cap rock zone that was thought to also fit with likely alteration zones (see Prasetyo, 2016 for details). Fig. 13 shows the shallow position of the clay cap. Deeper locations of the clay cap are shown in Fig. 14 and Fig. 15, which also shows the location of some faults.
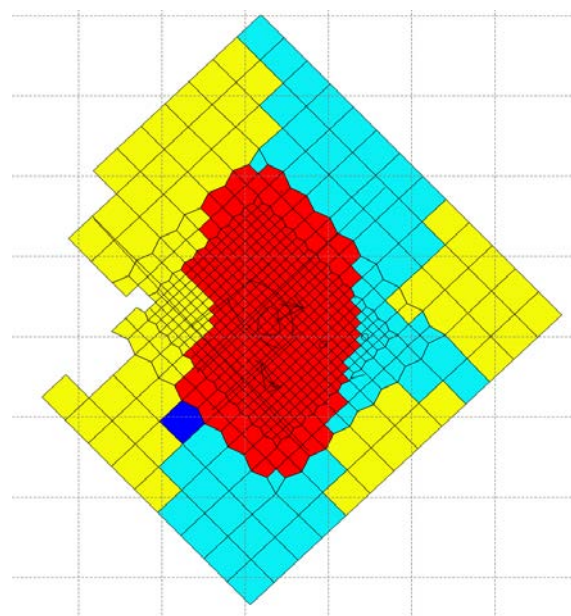
Figure 13: Cap rock (red) assignment on layer 10 (elevation 650 masl) for Model II

6
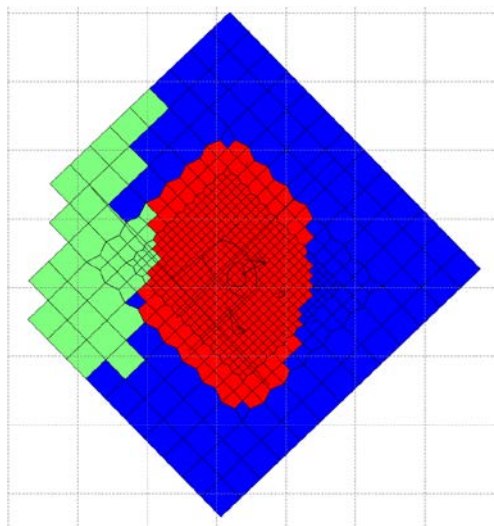
Figure 14: Cap rock (red) assignment on layer 11 (elevation 550 masl) for Model II
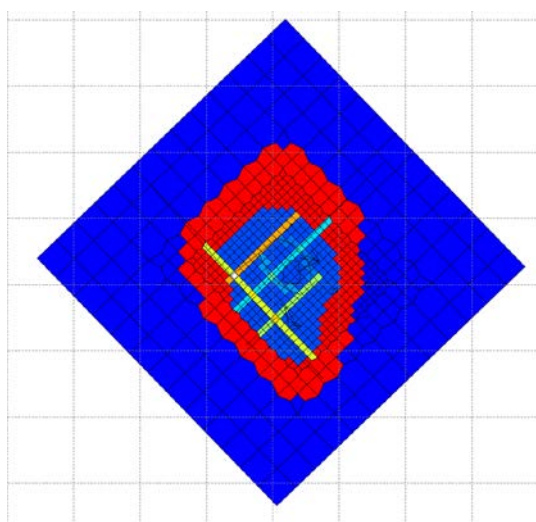
Figure 15: Cap rock (red) assignment on layer 13 (elevation 200 masl) for Model II

5.4   Model Calibration and Results

A brief manual calibration of Model II was conducted aiming to improve the goodness-of-fit to the data. iTOUGH2 was then used to further improve the match to the data. As shown in Table 1, after manual calibration the OF function for Model II was only marginally better than the value for the manually calibrated version of Model I.

Parameter estimation was performed on the values of permeabilities of the reservoir rock-types as well as the base inflows. The model has 86 rock types and, as mentioned above, in order to speed up the parameter estimation by iTOUGH2, the horizontal and lateral permeabilities were assumed to be linked ($k_x = k_y$), and therefore for Model II with 86 rock types, there were 172 permeability parameters to be estimated. Base inflows at 81 blocks were also selected as parameters to be estimated, giving a total of 253 adjustable model parameters. The bounds on all permeabilities were set at 1.0E-16 m^2 and 2.0E-12 m^2 and the bounds on inflows were set at 1.0E-6 kg/s and 10 kg/s. After one outer iteration of iTOUGH2, a k_x/k_y parameter with a low sensitivity was removed and that with a high sensitivity was split into separate k_x and k_y parameters, and

both further adjusted after the next outer iteration. The base inflows that were driven to the lower bound of 1.0E-6 kg/s were removed as parameters for further iTOUGH2 simulations and were fixed at the lower bound value.

Permeabilities that had moved to upper or lower bounds always had low sensitivities. They were left at the bounds or assigned reasonable values and then omitted from the calibration process.

Thus the following inverse modelling strategy was used:

(i)   Run one outer iteration of iTOUGH2
(ii)   Remove parameters with low sensitivities. For the permeabilities that reached an upper or lower bound leave at the bound or re-set to a reasonable value. For inflows that reached the lower bound remove as parameters and fix the value at the lower bound.
(iii) Update the remaining parameters
(iv)   Repeat (i)-(iii) until the OF is no longer decreasing significantly.

Temperature plots for the optimized version of Model II, comparing of the model results and measured data are shown in Figure 16. The OF for this model was 0.1030E6, a factor of 1.5 smaller than the OF for Model I.
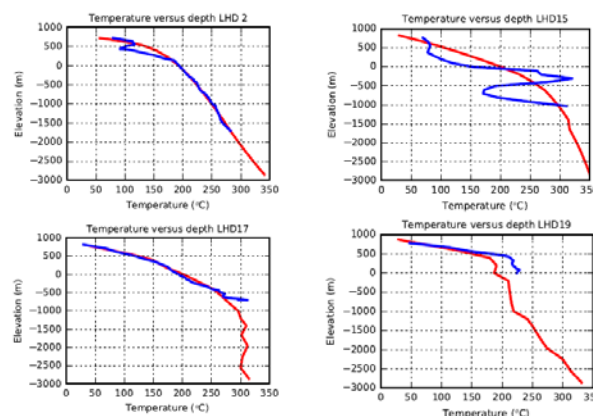
Figure 56: Model II temperature profiles for some wells after calibration with iTOUGH2

In the final iTOUGH2 simulation with Model II there were 91 permeability parameters and 45 mass inflow parameters, a total of 135, to be estimated (compared with 172 and 81, a total of 253 in the first iTOUGH2 Model II simulation).

The first iTOUGH2 simulation took ~ 7 days to complete whereas the final iTOUGH2 simulation took ~3 days. The run-time could have been reduced by using a parallel version of iTOUGH2.

6.   DISCUSSION AND CONCLUSION

The main objective of this study was to demonstrate the use of inverse modelling software for automated calibration of geothermal models. It was successfully applied to the improvement of a model of Lahendong geothermal field.

As a result of the study we have established a strategy for inverse modelling of geothermal fields that may be widely applicable. We recommend the following steps:

(i)   Set up a new conceptual model, either *ab initio* or by reviewing an existing conceptual model.

7

(ii)   Construct a computer model with a permeability structure and deep inflows that reflect the conceptual model

(iii) Use iTOUGH2 in the sequential, manual intervention mode (see Section 5.4) to optimise the model

(iv)   Assess the model fit and if desired repeat (i)-(iii). A re-design of the model grid may be required in each repetition of step (ii).

In our study Model I was the first iteration of the process summarised above and Model II was the second iteration. The process worked well as the objective function (the measure of goodness-of-fit of the model) was reduced from 0.2655E6 to 0.1030E6. By eye, the downhole temperature profiles can also be seen to be better matched. However the downhole temperature profiles are still not as good as we would expect to achieve with a thorough manual calibration exercise. Further iterations through our inverse modelling strategy are desirable. For example well LHD-15 (and some others not shown) shows evidence of a cold inflow. The conceptual model needs to be improved to explain how the cold inflow occurs and then a modified Model III should be set up and calibrated.

In theory, inverse modelling offers a fully automated alternative to manual calibration of geothermal models. However the strategy and protocols we discuss above require considerable manual input from expert geothermal modellers, reservoir engineers and geoscientists. If the conceptual model is not sufficiently detailed and the computer model structure is too simple there is a limit to how much inverse modelling can improve the model (as shown by the best version of our Model I).

Production history matching should also be included as part of the inverse modelling process to improve the model before it is ready for future production scenarios simulations, however for Lahendong good production history data are not available.

REFERENCES

Brehme, M., Moeck, I., Kamah, Y., Zimmermann, G. & Sauter, M.: A Hydrotectonic Model of a Geothermal Reservoir – A Study in Lahendong, Indonesia. *Geothermics,* 51, 228 – 239 (2014).

Brehme, M., Blocher, G., Cacace, M., Deon, F. Moeck, I., Wiegand, B., Kamah, Y., Regenspurg, S., Zimmermann, G., Sauter, M. & Huenges, E.: Characterizing permeability structures in geothermal reservoirs – A case study in Lahendong, Indonesia. *Proc. 41st Workshop on Geothermal Reservoir Engineering,* Stanford University, Stanford, California, *USA* (2016).

Brehme, M., Blocher, G., Cacace, M., Kamah, Y., Sauter, M. & Zimmermann, G.: Permeability distribution in the Lahendong geothermal field: A blind fault captured by thermal-hydraulic. *Environmental Earth Sciences,* 75:1088, 1-11 (2016).

Doherty, J.: *PEST: Model-Independent Parameter Estimation User Manual.* Watermark Numerical Computing (2005).

Finsterle, S.: *iTOUGH2 User's Guide,* Technical Report LBNL-40040 Rev.2, Earth Sciences Division, Lawrence Berkeley National Laboratory, University of California (2000).

Koestono, H., Siahaan, E.E., Silaban, M. & Franzson, H.: Geothermal Model of the Lahendong Geothermal Field, Indonesia. *Proc. World Geothermal Congress 2010,* Bali, Indonesia (2010).

O'Sullivan, M.J., Pruess, K. & Lippmann, M.J.: State of the art of geothermal reservoir simulation, *Geothermics*, 30, 395-429 (2001).

Prabowo, T., Yuniar, D.M., Suryanto, S. & Silaban, M.: Tracer Test Implementation and Analysis in Order to Evaluate Reinjection Effects in Lahendong Field. *Proc. World Geothermal Congress 2015*, Melbourne, Australia (2015).

Prasetyo, F.A.: *Inverse modelling of Lahendong geothermal field.* Master of Energy Report, University of Auckland (2016).

Raharjo, I.B., Maris, V., Wannamaker, P.E. & Chapman, D.S.: Resistivity Structures of Lahendong and Kamojang Geothermal Systems Revealed from 3-D Magnetotelluric Inversions, A Comparative Study. *Proc. World Geothermal Congress 2010*, Bali, Indonesia (2010)

Siahaan, E.E., Soemarinda, S., Fauzi, A., Silitonga, T., Azimudin, T., and Raharjo, I.B.: Tectonism and Volcanism Study in the Minahasa Compartment of the North Arm of Sulawesi Related to Lahendong Geothermal Field, Indonesia. *Proc. World Geothermal Congress 2005,* Antalya, Turkey (2005).

Sumantoro, Z.Z., Yeh, A., O'Sullivan, J.P. & O'Sullivan, M.J.: Reservoir Modelling of Lahendong Geothermal Field, Sulawesi – Indonesia. *Proc. 37th New Zealand Geothermal Workshop*, Wairakei, New Zealand (2015)

Utami, P., Siahaan, E.E., Azimudin, T., Suroto, Browne, P.R.L & Simmons, S.F.: Overview of the Lahendong Geothermal Field, North Sulawesi, Indonesia: a Progress Report. *Proc. 26th NZ Geothermal Workshop*, Auckland, New Zealand (2004).

Utami, P., Browne, P.R.L, Simmons, S.F & Suroto: Lahendong and some other geothermal systems in the Western Pacific belt: comparison on their geologic settings, hydrology and hydrothermal alteration. *Proc. 29th NZ Geothermal Workshop*, Auckland, New Zealand (2007).

Widagda, L. & Jagranatha, I.B.: Recahrge calculation of Lahendong Geothermal Filed in North Sulawesi – Indonesia. *Proc. World Geothermal Congress 2005,* Antalya, Turkey (2005).

Yani, A.: *Numerical Modeling of Lahendong Geothermal System, Indonesia.* Project Report: United Nations University-Geothermal Training Programme, Iceland (2006).

Yeh, A., Croucher, A. & O'Sullivan, M.: Recent Developments in the AUTOUGH2 Simulator. *Proc. TOUGH Symposium 2012,* Berkeley, California, USA (2012).

Yeh, A., Croucher, A. E., O'Sullivan, M.: TIM-Yet another graphical tool for TOUGH2. *Proc. 35th New Zealand Geothermal Workshop*, Rotorua, New Zealand (2013).

8